Hydrobiologia
November 2019, Volume 845, Issue 1, Pages 95-108
http://dx.doi.org/10.1007/s10750-018-3736-3
http://archimer.ifremer.fr/doc/00453/56476/

Size-effect, asymmetry, and small-scale spatial variation in otolith shape of juvenile sole in the Southern North Sea

Delerue-Ricard Sophie [1, 2, *], Hanna Stynen [1], Barbut Léo [1, 3], Morat Fabien [4, 5], Mahé Kelig [6], Hablützel Pascal [1], Hostens Kris [2], Volckaert Filip [1]

[1] Laboratory of Biodiversity and Evolutionary Genomics (LBEG), KU Leuven, Charles Deberiotstraat 32, Box 2439, 3000 Louvain, Belgium
[2] Institute for Agricultural and Fisheries Research, Ankerstraat 1, 8400 Ostend, Belgium
[3] Operational Directorate Natural Environment (OD Nature), Royal Belgian Institute of Natural Sciences (RBINS), Gulledelle 100, 1200 Brussels, Belgium
[4] PSL Research University: EPHE-UPVD-CNRS, USR3278 CRIOBE, 66860 Perpignan, France
[5] Laboratoire d'Excellence «CORAIL», BP 1013 Papetoai, 98729 Moore´a, French Polynesia
[6] Ifremer, Fisheries Laboratory, Sclerochronology Centre, 150 quai Gambetta, BP 699, 62321 Boulogne, France

* Corresponding author : Sophie Delerue-Ricard, email address : Sophie.DelerueRicard@kuleuven.be

Abstract :

While otolith shape analysis can provide a valuable tool for discriminating between fish populations, factors which may influence otolith shape, such as the effect of size, directional asymmetry in growth, and local environmental conditions, are often unknown. Here, we analyzed differences in otolith shape across three size classes of age-0 common sole *Solea solea* L. from nursery grounds off the Belgian coast and in the Wadden Sea. Across size classes, form-factor decreased and roundness remained consistently high in both nursery grounds, while ellipticity increased in the Belgian nursery. Directional asymmetry between left and right otoliths measured by Fourier coefficients accounted for 0.96 and 7.2% of the variance when comparing otoliths overall, and for each size class, respectively. Within the Belgian nursery, results were consistent across sampling years and locations. In addition, otolith shape was marginally different between nursery grounds, but highly variable within nursery grounds. A small divergent group, which seems partly related to fish size, was noted at both spatial and temporal scales. Based on these results and before embarking on a study of population structure using otolith shape in age-0 common sole, we recommend testing for directional asymmetry and fish size effects across the entire region of interest.

Keywords : Early-life stages, Fourier coefficients, Nursery ground, Otolith shape, Small-scale spatial structure

Introduction

Coastal ecosystems play a key role as nursery grounds for juvenile fish (Costanza et al., 1998) because of their high productivity. However, coastal nursery grounds have a discontinuous distribution, and experience increasing fragmentation due to anthropogenic pressures, which can result in changes of metacommunity diversity and dynamics (Jung et al., 2017). In addition, habitat heterogeneity within nursery grounds may influence the spatio-temporal dynamics of fish populations on a small spatial scale (Le Pape et al., 2003).

Various indirect methods are available to assess the spatial population dynamics of the early-life stages of marine fish, such as modelling of larval transport, comparison of parasite communities, analysis of genetic differentiation, chemical composition and shape of fish otoliths, or tagging of the late juvenile stages (Cadrin et al., 2014; Koubbi et al., 2006; Pawson & Jennings, 1996; Neves et al., 2018). Despite the diversity of methods, population structure and connectivity patterns between and within nursery grounds remain challenging to evaluate (Kaplan et al., 2016). Moreover, each tool may integrate information at specific, yet different spatial and temporal scales. Biophysical modelling of larval transport and otolith shape variation focus on 'ecological' time scales (Lacroix et al., 2013; Thorrold et al., 2001), while genomic tools have been applied to measure population structure over both short 'ecological' and longer 'evolutionary' time scales (Pinsky et al., 2017). Yet, advanced genomic tools work best with extensive genomic background information on the species of interest and well-preserved DNA.

Otoliths are calcified structures residing in the inner ear of fish, growing with the constant deposition of successive calcium carbonate layers. As they grow, otoliths incorporate time-delimited information that can be used to describe the development and ambient environmental conditions experienced by the individual. In addition, otolith shape is a useful and well-established tool to discriminate between species and stocks (Campana & Casselman, 1993). However, ontogenetic development affects otolith shape through changes in growth and metabolism, especially during

sexual maturity (Cardinale et al., 2004; Hüssy, 2008; Mérigot et al., 2007). During the early-life stages, otoliths evolve from circular to more complex shapes (Lagardère & Troadec, 1997; Hüssy, 2008), which may limit the utility of otolith shape as stock marker for immature fish or fish of different age classes. Moreover, left and right otoliths may be different, i.e. directionally asymmetrical, particularly in flatfishes (Mille et al., 2015). Environmental and anthropogenic pressure may cause stress-induced changes such as increased levels of directional asymmetry (Gagliano & McCormick, 2004), which is disadvantageous because it interferes with hearing and orientation (Anken et al., 2002; Lychakov & Rebane, 2005).

Most studies have compared intraspecific differences in otolith shape either over large distances (>500 km e.g. Vieira et al., 2014), across oceanographic barriers (Tuset et al., 2003) or between habitats (Morat et al., 2014; Vignon & Morat, 2010). It is not yet clear what can be learned from otolith shape at small spatial scales and in the absence of strong oceanographic barriers. Here we used otolith shape analysis to investigate small-scale nursery structure of the flatfish sole *Solea solea* (Linnaeus, 1758; Soleidae) in the shallow subtidal of the Southern North Sea. Sole is less abundant than European plaice (*Pleuronectes platessa* L.) or dab (*Limanda limanda* L.*)* in the study area, but it has a high commercial value, contributing to important regional and local demersal fisheries. To date, connectivity patterns between spawning and nursery grounds remain unclear (Burt & Millner, 2008; Lacroix et al., 2013). In the Southern North Sea, sole displays peak spawning from April to June. After hatching the pelagic larvae drift for ~1 month in the water column before settling in a nursery (Russell, 1976; van der Land, 1991). Genetic data from adult sole suggest isolation by distance along the Atlantic coast, and weak population structure within the Southern North Sea (Cuveliers et al., 2012; Diopere et al., 2018), with a mean dispersal distance estimated at 150 km (Kotoulas et al., 1995; Lacroix et al., 2013). Within the nursery grounds, age-0 sole travel shorter distances, between 10 and 30 km (Le Pape & Cognez, 2016). Nevertheless, small-scale spatio-temporal variation in connectivity between and within nursery grounds has, to the best of our knowledge, not been investigated empirically. The degree of isolation between and within nursery grounds may be estimated from the variation in otolith shape. Being able

to delineate the smallest level of spatial resolution is an important step to measure connectivity and to better understand recruitment patterns.

In the current study we addressed three key questions to determine whether otolith shape can be used to assess small-scale spatial patterns in juvenile flatfish: (1) what is the effect of fish size on otolith shape; (2) what is the effect of directional asymmetry between left and right otoliths, and (3) whether is there spatio-temporal variation in the otolith shape of age-0 sole.

Material and methods

We investigated variation in otolith shape over two years and at two spatial scales within the dispersal range of sole larvae, to better understand the resolution of otolith shape variation between and within nursery grounds in the Southern North Sea. Juvenile sole were sampled at the regional scale (between nursery grounds, 400 km distance) from the Belgian and Wadden Sea nursery grounds in 2014 (NL2014 and BE2014). Juvenile sole were sampled at the local scale (within nursery) from the eastern and the western shallow subtidal coastal zones of the Belgian nursery in 2013 and 2014 (BE2013 and BE2014, 40 km distance between coastal zones). The discriminatory power of otolith shape was tested using Fourier coefficients and shape indices (see further). In addition, asymmetry between left and right otoliths and correlations between the shape indices and fish size were estimated using the combined data from all fish from the three datasets (BE2013, BE2014, NL2014).

Sample collection

Juvenile sole were sampled off the Belgian coast from late August to late September in 2013 and from mid-September to mid-October in 2014 (Figure 1; Table 1) and at two stations in the Wadden Sea in September 2014. At each site, specimens were collected by beam trawling either on board of RV *Simon Stevin* (B-FishConnect project campaign), RV *Belgica* (Belgian Demersal Young Fish Survey, DYFS) or RV *Stern* (Dutch DYFS). Sea surface temperature was measured at each site at the time of collection. Each

fish was measured to the nearest mm (Standard Length, SL). Sagittal otoliths were extracted from a total of 314 individuals ranging from 52 to 102 mm SL. Finally, each otolith was cleaned, sonicated, and then stored dry in plastic vials. For this study, age-0 sole were used. Fish age was confirmed by the absence of an annual ring in the otolith. To assess variation in otolith shape associated with fish size, the 314 individuals were divided into three standard length size-classes, L1 (52-76 mm, n = 105), L2 (76-82 mm, n = 105) and L3 (82-102 mm, n = 104).

Otolith shape indices and Fourier coefficients

Left and right sagittae were placed on a microscope slide with a black background, positioned with the *sulcus acusticus* oriented towards the observer and the posterior side oriented to the top. External transmitted light sources were used and adjusted to illuminate the otoliths. High-contrast images were produced using an Olympus ColorView digital microscope camera linked to an Olympus BX51 microscope (20x magnification). Images were then processed with the TNPC 7 software ('Digital Processing for Calcified Structures'; www.tnpc.fr) to extract the following morphometric parameters: surface area of the otolith (A_o); otolith perimeter (P_o); maximum length (L_o); and width (O_w) to the nearest 10^{-2} mm. Based on these measurements, form-factor, roundness, circularity, rectangularity, and ellipticity were calculated as in Tuset et al. (2003). Form-factor estimates surface area irregularity and has a maximal value of one in the case of a perfect circle. Roundness and circularity describe the proximity of shape to a circle and have minimal values of one and 12.57, respectively. The closer both indices approach the minimal value, the closer the shape of the otolith is to a perfect circle. Rectangularity gives the proportion of the length and width with respect to the area and has a maximal value of one in case of a perfect square. Ellipticity describes the proportion of change in the different axes (Tuset et al., 2003).

In addition to the use of shape indices, otolith contours were described by Elliptic Fourier Descriptors (EFDs) which were obtained with TNPC 7 software. For each otolith, the first 99 elliptical

Fourier harmonics were extracted and normalised with respect to the first harmonic. Hence, they were invariant to otolith size, rotation and starting point of the contour description (Kuhl & Giardina, 1982). To determine the number of elliptical Fourier harmonics required to reconstruct the otolith outline, the Fourier Power (FP) spectrum was calculated for each individual otolith. For the n^{th} harmonic, Fourier Power is given by the equation:

$$FP_n = ({A_n}^2 + {B_n}^2 + {C_n}^2 + {D_n}^2)/2,$$

where A_n , B_n , C_n and D_n are the Fourier coefficients of the n^{th} harmonic.

Cumulative Fourier Power (FP_c) was calculated by summing the Fourier power of each harmonic:

$$FP_c = \sum_1^n FP_n$$

The number of harmonics was chosen such that the mean cumulated FP reached 99.99%; hence shape was reconstructed at 99.99% (Mérigot et al., 2007; Gonzalez-Salas & Lenfant, 2007). The first harmonic was not considered for further analysis (except for reconstructing average shape), because it had already been used for normalization, and because it would dominate shape reconstruction and mask the information derived from the other harmonics (Crampton, 1995).

Statistical analysis

First, a pilot experiment was conducted to assess the consistency of our methodology with regard to otolith position and lighting. Ten randomly chosen otoliths were repositioned and four replicate pictures were taken. A dendrogram analysis was performed to test the extent of differences between images of the same otolith and differences between images of different otoliths.

Multi-collinearity between shape indices was assessed by Pearson correlation. Only form-factor, roundness and ellipticity were kept for further analyses. Shape indices were compared between length classes, the two nursery grounds, and sampling years. Differences in the mean values of shape indices

between each size class and each dataset were assessed using non-parametric *k*-sample Anderson-Darling tests under the null hypothesis that all samples originated from the same distribution.

Before analyzing asymmetry levels and spatio-temporal variation in the Fourier coefficients, Principal Component Analysis (PCA) was applied to the Fourier coefficients to avoid collinearity of shape descriptors, and to reduce the number of dimensions while retaining the majority of the variance (Rohlf & Archie, 1984). Only PCs with eigenvalues higher than the mean of all eigenvalues were retained to remove Principal Components (PCs) associated with noise. Fourier coefficients were significantly correlated with fish size. Residuals of the PCs of Fourier coefficients have been used to remove the effect of fish size, as in Mahé et al. (2016).

Partial Redundancy Analysis (pRDA) tests were performed with the PCs of the Fourier coefficients as response variables to explore the effect of otolith side, between and within-nursery spatial variation, year, coastal region and Sea Surface Temperature (SST). Redundancy analysis is an extension of multiple regression analysis to multivariate response data (Legendre & Legendre, 2012). In all pRDAs, SL was used to correct for fish size, and a permutation test was used to assess the significance of the explanatory variables. A pRDA was performed to test the effect of otolith side (left/right) on shape. To visualize and quantify differences between left and right otoliths, the average otolith shape of each side was also built by outline reverse Fourier transformation, as in Mille et al. (2015).

Dendrograms were produced by ascending hierarchical classification (AHC) to verify the PCA clustering of individuals at the regional and local scales. AHC maximizes the similarities within clusters and differences between clusters of similar otolith shapes. To compute the AHC, the function 'HCPC' based on Ward's distance was used.

pRDA was also used to determine regional and local scale (between and within nursery) annual differences in otolith shape. We used multiple linear regressions to test at the regional scale the effect of nursery, sampling date, and SST on the Fourier coefficient PCs, and to test at the local scale the

effect of year, coastal zone (eastern/western), and SST on the same PCs. We determined the variance explained by each explanatory variable. Only the left otoliths were used in the RDAs. Distribution of standard length was compared using a randomization test. All statistical analyses were performed using the *ade4*, *FactoMineR*, *vegan* and *stats* packages in the statistical environment R (R Development Core Team, 2011).

The outlines of the mean Fourier coefficients (prior to size correction) were plotted as an overlay image to visualize differences in otolith shape between left and right otoliths. The same overlay was used to visualize differences between left otoliths of the Belgian and Wadden Sea nursery grounds, and between left otoliths of the two PCA clusters (Mille et al., 2015).

Results

Cluster analysis showed that Fourier coefficients extracted from replicated images of the same otolith were consistently grouped together and our measures were accurate (Supplementary Figure S1). Otolith form-factor, ellipticity and roundness were not redundant (Pearson correlation test, $P > 0.05$) and were kept for further analysis. For each dataset (BE2013, BE2014 and NL2014), form-factor significantly decreased with increasing standard length (Figure 2a; Table 2). Only in the Belgian nursery ellipticity was significantly different between length classes for both sampling years (Figure 2b). Roundness was generally close to one and did not vary significantly between size classes or nursery grounds but varied between sampling years in the Belgian nursery (Supplementary Figure S2). In addition, otoliths sampled in 2014 off the Belgian coast were significantly more circular than in the Wadden Sea, and also significantly more circular and rounder than otoliths sampled in 2013 on the Belgian nursery as shown by form-factor variations (Table 2).

The Fourier coefficients differed significantly between left and right otoliths (n = 314, $P < 0.01$). This directional asymmetry explained almost 6% of the variance (Table 3) and was spread homogeneously across the otolith outline (Figure 3a). Although the overall average directional

asymmetry was quite small when all datasets and size classes were pooled (0.96% overall), asymmetry was much higher when each dataset and size classes were examined separately (mean asymmetry for each dataset was 7.2%). Left otoliths of sole (blind side) were larger than right otoliths (eyed-side) and were thus kept for further analysis.

Among the 99 Fourier harmonics extracted to describe the left otolith contour, the first 22 harmonics explained more than 99.99% of the variance and were thus retained for multivariate analyses. Small differences in average shape (1.2% overall) were visible between the Belgian and Wadden Sea nursery grounds based on the reconstructed average otolith shape (Figure 3b). The variance in otolith shape explained by fish size (P = 0.086 and P = 0.004 for NL-BE 2014 and BE 2013-2014, respectively) was removed (see Material and methods section Statistical analysis for more details). The first and second axes from a PCA comparing the Belgian and Wadden Sea nursery grounds in 2014 accounted for 30.2 and 28.6% of the total variance, respectively. At the local scale (within the Belgian nursery) in 2013 and 2014, the first and second PCs accounted for 31.8 and 28.6% of the total variance, respectively. Ten PCs had eigenvalues above the mean eigenvalue, and accounted for 91.0% of the variance when comparing shapes at both nursery grounds in 2014, and 90.6% when comparing shapes in the Belgian nursery between years. Both PCA plots showed considerable variation in otolith shape both at the regional and local scale, and it was not possible to detect PCA clusters by nursery or by year (Figure 4a and 4b). However, two distinct clusters were observed at both geographical scales and during both sampling years based on the first two PCs. These clusters were also supported in both cases by clustering dendrograms (Supplementary Figure S3). A small number of fish, belonging to both the Belgian and Wadden Sea nursery grounds (Figure 4a) and both 2013 and 2014 Belgian samples (Figure 4b), clearly diverged in otolith shape. This divergent group of fish consisted of approximately 10% of the individuals from NL2014, 10% of BE2014 and 16% of the BE2013, independent of standard length size class. Shape diverged in two areas on both the posterior or anterior side of the otolith and accounted for 11.5% of shape variation (Figure 3c). For the 2014 dataset, fish from the divergent group were significantly longer (SL: 72 to 95 mm) than those from the majority cluster (SL: 57 to 93 mm)

246 (Figure 5; randomization test for NL-BE 2014: n = 141, W = 1221, *P* = 0.041). In the Belgian nursery, the
247 average SL of the divergent group was not significantly longer than that of the majority cluster for the
248 local dataset (Figure 5; randomization test for BE 2013-2014: n = 253, W = 4258, *P* = 0.525).

249 Redundancy analysis (RDA) was used to correlate the observed pattern of otolith shape with
250 potential explanatory variables (Table 3). At the regional scale, otolith shapes in the Belgian and
251 Wadden Sea nursery grounds differed significantly, even though that difference was only marginally
252 significant (*P* = 0.04) and explained less than 1% of the variance. At the local scale of the Belgian
253 nursery, neither an effect of sampling year nor of coastal zone (eastern/western) on otolith shape was
254 detected. Both SST and sampling date did not significantly explain variation in otolith shape,
255 irrespective of the spatial scale considered.

256

257 **Discussion**

258 Analysis of otolith shape on age-0 sole collected in the Southern North Sea revealed five interesting
259 results. Otolith shape, as described by shape indices and Fourier coefficients, was influenced by fish
260 size. Weak but significant directional asymmetry in otolith shape was observed between the left and
261 right otoliths. Among-site variation in otolith shape was small but significant at the regional scale
262 (Belgian vs. Wadden Sea nursery grounds, 400 km distance). Such variation was absent at the local
263 scale (eastern vs. western coastal zones of the Belgian nursery, 40 km distance) and between two
264 consecutive years (2013 vs. 2014).

265

266 Impact of fish size and directional asymmetry on shape in age-0 sole

267 Several confounding factors were taken into account before considering which factors drive spatial
268 and temporal variation of otolith shape. First of all, a single age group (age-0 sole) was considered.
269 Secondly, we corrected Fourier coefficients for fish size (Campana & Casselman, 1993; Cardinale et al.,

2004; Mérigot et al., 2007). Thirdly, variation due to methodology and individual variability was successfully addressed in a pilot experiment focusing on positioning and lighting methods of the photography.

Adult otoliths tend to be more complex in shape than juvenile otoliths (Capoccioni et al., 2011; Morat et al., 2017). Directional asymmetry in shape, mass and chemical composition have been observed between the left and right otoliths in adult and juvenile flatfish but never quantified in juveniles (Mille et al., 2015; Mérigot et al., 2007). This study demonstrates that directional asymmetry is already present in age-0 flatfish. Our results suggest that asymmetry builds up over time because of differential growth between the larger otolith on the blind side vs. the smaller otolith on the eyed side. Still, the limited variation observed between both otolith sides supports Mille et al. (2015) suggestion of the presence of an evolutionary selection pressure against asymmetry to avoid negative effects on fish hearing and equilibrium.. Our study establishes that, similarly to adults (Mille et al., 2015), left and right otoliths should not be used interchangeably in shape analyses of juvenile sole. This lack of interchangeability is likely for all other analyses carried out on otoliths, such as chemical asymmetry (Morat et al., 2014). Moreover, fish size should always be accounted for because it affects otolith shape even in age-0 fish. Our results are consistent with Mapp et al. (2017), who showed that including size information increases the power of stock discrimination based on juvenile otolith shape. The form-factor decreased with increasing size in both nursery grounds and during both sampling years, while ellipticity increased in the Belgian nursery. Roundness did not vary significantly either with fish size or between nursery grounds. The only difference in roundness we could detect was in the Belgian nursery, where roundness was lower in 2013 than in 2014. Overall, roundness was higher than observed in Mediterranean samples (Mérigot et al., 2007), which might be due to higher growth rates in the Mediterranean Sea compared to the North Sea sole (Morat, 2011). In summary, we show that otoliths of age-0 sole in the Southern North Sea were relatively round, directionally asymmetrical, and that area irregularity increased during the first year of life.

296 Small differences between nursery grounds

297 Our results show that we can detect variation in otolith shape at relatively small spatial scales. Overall,
298 the average shape differed more between nursery grounds than between otolith sides, although these
299 differences disappear when size classes are taken into account and asymmetry measured within each.
300 This result suggests that differences between nursery grounds are size related. Assuming comparable
301 environmental conditions at the Belgian and Wadden Sea nursery grounds (OSPAR, 2000), one might
302 expect a comparable nursery ground environment impact on otolith shape, which we do not observe.
303 Thus other factors, such as genetic background, spawning location and dispersal may also be important
304 in influencing otolith shape (Cardinale et al., 2004; Capoccioni et al., 2011; Lombarte et al., 2003; Mapp
305 et al., 2017). This observation is supported by the similar levels of variation in otolith shape between
306 nursery grounds and between the two successive sampling years. Genetic levels are expected to vary
307 only to a limited extent within the Southern North Sea, because sole exhibit an almost homogeneous
308 population structure (Cuveliers et al., 2012; Diopere et al., 2018). At the same time, earlier
309 microchemical studies point to a reduced mobility and site fidelity of age-0 sole in the Southern North
310 Sea (Cuveliers et al., 2010; Le Pape & Cognez, 2016). Differences in otolith shape and microchemistry
311 between two 'adjacent' nursery grounds support some degree of natal site fidelity, which is not
312 unexpected given the temporally stable location of the spawning grounds of sole.

313

314 A divergent group of age-0 sole at both nursery grounds

315 We noticed two distinct groups of otolith shapes in both PCA analyses and clustering dendrograms.
316 This result raises the question as to whether these individuals, representing 10 and 16% of all age-0
317 sole screened respectively, experienced a somewhat different environment or have a different origin.
318 Fish of the divergent group exhibited a larger size than most other fish. However, the divergent group
319 was sampled across sampling dates (spanning over one month), suggesting that shape differences are
320 not linked to age differences between individuals.

The environmental conditions experienced during juvenile dispersal depend on spawning ground and planktonic drift. According to the biophysical model of Lacroix et al. (2013), larvae arriving at the Belgian and Wadden Sea nursery grounds originate from the spawning grounds off the Belgian coast, the Eastern English Channel and the Thames Estuary. Between-year connectivity levels are comparable, although the relative proportions of source populations vary. Building on the results of the present study, other approaches would be required to identify larval origin. For example, spawning time can be estimated from otolith microstructure and used to back-calculate larval origin (Amara et al., 1993). Shape differences might be related to residence time on the nursery ground (Delerue-Ricard in prep.). Additionally, otolith microchemistry is effective in resolving small-scale spatial differences. Based on otolith microchemistry, Cuveliers et al. (2010) were able to distinguish nursery grounds of sole from the Thames Estuary, Belgian coast, and Wadden Sea. However, chemical signatures of spawning grounds of sole in that area have yet to be explored. In summary, complementary information on otolith chemistry, biophysical modeling or a combination using the aforementioned techniques, should reveal the origin of spawning, and the dispersal pathways (Campana, 2005; Morat et al., 2014). Such information would contribute to a better understanding of the connectivity patterns of sole between spawning and nursery grounds.

The importance of spatial scale

Understanding local population dynamics is crucial, especially for coastal habitats, which are key nursery grounds for many marine species. Over the last decades changes in food webs and sheltering conditions provided by structuring benthos have dramatically affected nursery function along the North Sea coast (Jung et al., 2017; Rabaut et al., 2013; Van der Veer et al., 2011). We examined otolith shape across the Southern North Sea at a scale close to the average dispersal distance of sole (150 km, Kotoulas et al., 1995). Small, but significant differences were identified between two adjacent nursery grounds. Within each nursery ground, no differences in otolith shape were found, despite differences

346 in habitat characteristics between the eastern and the western coastal zones of the Belgian nursery,
347 with mostly muddy to sandy sediments in the east and sandy to muddy sediments in the west (Van
348 Hoey et al., 2004). Each sediment type harbors a specific macrobenthic assemblage (Degraer et al.,
349 2008; Rabaut et al., 2013), with a distinct prey spectrum for sole and potential influence on otolith
350 shape. However, starvation experiments suggest that food quantity could be more important than
351 food type to determine otolith shape. Thus, if juvenile sole would be restricted to one coastal nursery
352 ground or region within the Belgian nursery, the limited effect of food type on otolith shape could
353 partially explain the absence of variation within the Belgian nursery (Cardinale et al., 2004; Gagliano &
354 McCormick, 2004; Hüssy, 2008).

355 In conclusion, small scale differences in otolith shape can be diagnostic and may play a role in
356 population dynamic studies. During the first year of life of sole, otolith shape evolves from round to a
357 more complex shape. Directional asymmetry between left and right otoliths is already present in age-
358 0 sole and has therefore to be taken into account in flatfish juveniles and adults alike. Despite a large
359 variation in otolith shape, a subtle but significant difference was observed at a scale of 400 km, i.e. the
360 dispersal scale of sole, which is a promising finding for the study of small-scale spatial patterns. At the
361 local scale (within nursery grounds), no significant shape differences were noted between the eastern
362 and the western coastal zones of the Belgian nursery, nor between 2013 and 2014. However, a number
363 of samples showing a divergent otolith shape, probably linked to fish size, was found on both nursery
364 grounds in both successive years. Complementary studies on the integration of high resolution
365 genotyping, elemental analysis of otoliths and biophysical modelling of early-life stages, are expected
366 to provide additional evidence on the dispersal dynamics between spawning and nursery grounds.

367

368

369 **Acknowledgments**

Special thanks to K. Vanhalst (Institute for Agricultural and Fisheries Research, ILVO), the crew of RV *Simon Stevin* and RV *Belgica*, L. Bolle (Wageningen Marine Research), the crew of RV *Stern* and the B-FishConnect team for sampling. We are grateful to E. De Keyser, H. Christiansen, F. M. Heindler, F. Calboli (KU Leuven), B. Ernande (Ifremer), G. Lacroix (Royal Belgian Institute of Natural Sciences, RBINS), A. Vanden Bavière, J. Robbens (ILVO) and M. R. Siskey (Stony Brook University) for constructive comments. The B-FishConnect project was funded by the Research Foundation – Flanders (project number G.0702.13N). Thanks also to three anonymous reviewers, who provided many helpful comments.

Data availability

The datasets generated and analyzed during the current study are available from the corresponding author on reasonable request.

References

Amara, R., F. Lagardère, & Y. Desaunay, 1993. Seasonal distribution and duration of the planktonic stage of Dover sole, *Solea solea*, larvae in the Bay of Biscay: an hypothesis. Journal of Fish Biology 43: 17–30.

Anken, R. H., M. Beier, & H. Rahmann, 2002. Influence of hypergravity on fish inner ear otoliths: I. Developmental growth profile. Advances in Space Research 30: 721–725.

Burt, G. J., & R. S. Millner, 2008. Movements of sole in the southern North Sea and eastern English Channel from tagging studies (1955–2004). Science Series Technical Report. Cefas Lowestoft, 143: 1–44

394 Cadrin, S. X., A. L. Kerr, & S. Mariani (eds), 2014. Stock identification methods: applications in fishery
395 science. Academic Press, Amsterdam.

396 Capoccioni, F., C. Costa, J. Aguzzi, P. Menesatti, A. Lombarte, & E. Ciccotti, 2011. Ontogenetic and
397 environmental effects on otolith shape variability in three Mediterranean European eel (*Anguilla*
398 *anguilla,* L.) local stocks. Journal of Experimental Marine Biology and Ecology 397: 1–7.

399 Campana, S. E., 2005. Otolith elemental composition as a natural marker of fish stocks. In Stock
400 identification methods (eds), Academic Press, Burlington: 227–245

401 Campana, S. E., & J. M. Casselman, 1993. Stock discrimination using otolith shape analysis. Canadian
402 Journal of Fisheries and Aquatic Sciences 50: 1062–1083.

403 Cardinale, M., P. Doering-Arjes, M. Kastowsky, & H. Mosegaard, 2004. Effects of sex, stock, and
404 environment on the shape of known-age Atlantic cod (*Gadus morhua*) otoliths. Canadian Journal of
405 Fisheries and Aquatic Sciences 61: 158–167.

406 Costanza, R., R. d'Arge, R. De Groot, S. Farber, M. Grasso, B. Hannon, K. Limburg, S. Naeem, R. V.
407 O'Neill, J. Paruelo, R. J. Raskin, P. Sutton, & M. van den Belt, 1998. The value of ecosystem services:
408 putting the issues in perspective. Ecological Economics 25: 67–72.

409 Crampton, J. S., 1995. Elliptic Fourier shape analysis of fossil bivalves: some practical considerations.
410 Lethaia 28: 179–186.

411 Cuveliers, E., A. Geffen, J. Guelinckx, J. Raeymaekers, J. Skadal, F. Volckaert, & G. Maes, 2010.
412 Microchemical variation in juvenile *Solea solea* otoliths as a powerful tool for studying connectivity in
413 the North Sea. Marine Ecology Progress Series 401: 211–220.

414 Cuveliers, E. L., M. H. D. Larmuseau, B. Hellemans, S. L. N. A. Verherstraeten, F. A. M. Volckaert, & G.
415 E. Maes, 2012. Multi-marker estimate of genetic connectivity of sole (*Solea solea*) in the North-East
416 Atlantic Ocean. Marine Biology 159: 1239–1253.

417 Degraer, S., E. Verfaillie, W. Willems, E. Adriaens, M. Vincx, & V. Van Lancker, 2008. Habitat suitability
418 modelling as a mapping tool for macrobenthic communities: An example from the Belgian part of the
419 North Sea. Continental Shelf Research 28: 369–379.

420 Diopere, E., Cariani, A., Vandamme, S., Van Houdt, J., Tinti, F., Volckaert, F.A.M., FISHPOPTRACE
421 Consortium & G.E., Maes, 2018. Seascape genetics of a flatfish reveals local selection under high levels
422 of gene flow. ICES Journal of Marine Science 75: 675–689.

423 Gagliano, M., & M. I. McCormick, 2004. Feeding history influences otolith shape in tropical fish. Marine
424 Ecology Progress Series 278: 291–296.

425 Gonzalez-Salas, C., & P. Lenfant, 2007. Interannual variability and intraannual stability of the otolith
426 shape in European anchovy *Engraulis encrasicolus* (L.) in the Bay of Biscay. Journal of Fish Biology 70:
427 35–49.

428 Hüssy, K., 2008. Otolith shape in juvenile cod (*Gadus morhua*): Ontogenetic and environmental effects.
429 Journal of Experimental Marine Biology and Ecology 364: 35–41.

430 Jung, A., R. Dekker, M. Germain, C. Philippart, J. Witte, & H. van der Veer, 2017. Long-term shifts in
431 intertidal predator and prey communities in the Wadden Sea and consequences for food requirements
432 and supply. Marine Ecology Progress Series 579: 37–53.

433 Kaplan, D. M., M. Cuif, C. Fauvelot, L. Vigliola, T. Nguyen-Huu, J. Tiavouane, & C. Lett, 2017. Uncertainty
434 in empirical estimates of marine larval connectivity. ICES Journal of Marine Science 74: 1723–1734.

435 Kotoulas, G., F. Bonhomme, & P. Borsa, 1995. Genetic structure of the common sole *Solea vulgaris* at
436 different geographic scales. Marine Biology 122: 361–375.

437 Koubbi, P., C. Loots, G. Cotonnec, X. Harlay, A. Grioche, S. Vaz, C. C. C. U. Martin, M. Walkey, & A.
438 Carpentier, 2006. Spatial patterns and GIS habitat modelling of *Solea solea*, *Pleuronectes flesus* and
439 *Limanda limanda* fish larvae in the eastern English Channel during the spring. Scientia Marina 147–
440 157.

441 Kuhl, F. P., & C. R. Giardina, 1982. Elliptic Fourier features of a closed contour. Computer Graphics and
442 Image Processing 18: 236–258.

443 Lacroix, G., G. E. Maes, L. J. Bolle, & F. A. M. Volckaert, 2013. Modelling dispersal dynamics of the early
444 life stages of a marine flatfish (*Solea solea* L.). Journal of Sea Research 84: 13–25.

445 Lagardère, F., & H. Troadec, 1997. Age estimation in common sole *Solea solea* larvae: validation of
446 daily increments and evaluation of a pattern recognition technique. Marine Ecology Progress Series
447 155: 223–237.

448 Legendre, & Legendre (eds), 2012. Numerical Ecology, Volume 24 – Elsevier. 1006 pp.

449 Le Pape, O., F. Chauvet, S. Mahévas, P. Lazure, D. Guérault, & Y. Désaunay, 2003. Quantitative
450 description of habitat suitability for the juvenile common sole (*Solea solea*, L.) in the Bay of Biscay
451 (France) and the contribution of different habitats to the adult population. Journal of Sea Research 50:
452 139–149.

453 Le Pape, O., & N. Cognez, 2016. The range of juvenile movements of estuarine and coastal nursery
454 dependent flatfishes: estimation from a meta-analytical approach. Journal of Sea Research 107: 43–
455 55.

456 Lombarte, A., G. J. Torres, & B. Morales-Nin, 2003. Specific Merluccius otolith growth patterns related
457 to phylogenetics and environmental factors. Journal of the Marine Biological Association of the UK 83:
458 277–281.

459 Lychakov, D. V., & Y. T. Rebane, 2005. Fish otolith mass asymmetry: morphometry and influence on
460 acoustic functionality. Hearing Research 201: 55–69.

461 Mahé, K., C. Oudard, T. Mille, J. Keating, P. Gonçalves, L. W. Clausen, G. Petursdottir, H. Rasmussen, E.
462 Meland, E. Mullins, J. K. Pinnegar, Å. Hoines, & V. M. Trenkel, 2016. Identifying blue whiting
463 (*Micromesistius poutassou*) stock structure in the Northeast Atlantic by otolith shape analysis.
464 Canadian Journal of Fisheries and Aquatic Sciences 73: 1363–1371.

465 Mapp, J., E. Hunter, J. Van Der Kooij, S. Songer, & M. Fisher, 2017. Otolith shape and size: The
466 importance of age when determining indices for fish-stock separation. Fisheries Research 190: 43–52.

467 Mérigot, B., Y. Letourneur, & R. Lecomte-Finiger, 2007. Characterization of local populations of the
468 common sole *Solea solea* (Pisces, Soleidae) in the NW Mediterranean through otolith morphometrics
469 and shape analysis. Marine Biology 151: 997–1008.

470 Mille, T., K. Mahé, M. C. Villanueva, H. De Pontual, & B. Ernande, 2015. Sagittal otolith morphogenesis
471 asymmetry in marine fishes. Journal of Fish Biology 87: 646–663.

472 Morat, F., 2011. Influence des apports rhodaniens sur les traits d'histoire de vie de la sole commune
473 (*Solea solea*) : apports de l'étude minéralogique et chimique des otolithes. Thèse de doctorat,
474 spécialité Océanographie, Université Aix Marseille II, Marseille, France, 308 pp

475 Morat, F., Gibert, P., Reynaud, N., Testi, B., Favriou, P., Raymond, V., Carrel, G. & Maire, A., 2017.
476 Spatial distribution, total length frequencies and otolith morphometry as tools to analyse the effects
477 of a flash flood on populations of roach (*Rutilus rutilus*). Ecology of Freshwater Fish 27: 421–432.

478 Morat, F., Y. Letourneur, J. Dierking, C. Pécheyran, G. Bareille, D. Blamart, & M. Harmelin-Vivien, 2014.
479 The great melting pot. Common sole population connectivity assessed by otolith and water
480 fingerprints. PLOS ONE 9 (1): e86585.

481 OSPAR Commission (eds), 2000. Region 2: Greater North Sea. London.

482 Neves, V., D. Silva, F. Martinho, C. Antunes, S. Ramos, & V. Freitas, 2018. Assessing the effects of
483 internal and external acoustic tagging methods on European flounder *Platichthys flesus*. Fisheries
484 Research 206: 202–208.

485 Pawson, M. G., & S. Jennings, 1996. A critique of methods for stock identification in marine capture
486 fisheries. Fisheries Research 25: 203–217.

487 Pinsky, M. L., P. Saenz-Agudelo, O. C. Salles, G. R. Almany, M. Bode, M. L. Berumen, S. Andréfouët, S.
488 R. Thorrold, G. P. Jones, & S. Planes, 2017. Marine dispersal scales are congruent over evolutionary
489 and ecological time. Current Biology 27: 149–154.

490 R development core team. 2011. R: A language and environment for statistical computing. R
491 Foundation for Statistical Computing, Vienna, Austria.

492 Rabaut, M., M. Audfroid Calderón, L. Van de Moortel, J. van Dalfsen, M. Vincx, S. Degraer, & N. Desroy,
493 2013. The role of structuring benthos for juvenile flatfish. Journal of Sea Research 84: 70–76.

494 Rohlf, F. J., & J. W. Archie, 1984. A comparison of Fourier methods for the description of wing shape in
495 mosquitoes (Diptera: Culicidae). Systematic Biology 33: 302–317.

496 Russell, F. S. (eds), 1976. The eggs and planktonic stages of British marine fishes. Academic Press,
497 London, New York, 524 pp.

498 Thorrold, S. R., C. Latkoczy, P. K. Swart, & C. M. Jones, 2001. Natal homing in a marine fish
499 metapopulation. Science (New York, N.Y.) 291: 297–299.

500 Tuset, V. M., I. J. Lozano, J. A. González, J. F. Pertusa, & M. M. García-Díaz, 2003. Shape indices to
501 identify regional differences in otolith morphology of comber, *Serranus cabrilla* (L., 1758). Journal of
502 Applied Ichthyology 19: 88–93.

503 Van der Land, M. A., 1991. Distribution of flatfish eggs in the 1989 egg surveys in the southeastern
504 North Sea, and mortality of plaice and sole eggs. Netherlands Journal of Sea Research 27: 277–286.

505 Van der Veer, H., J. Koot, G. Aarts, R. Dekker, W. Diderich, V. Freitas, & J. Witte, 2011. Long-term trends
506 in juvenile flatfish indicate a dramatic reduction in nursery function of the Balgzand intertidal, Dutch
507 Wadden Sea. Marine Ecology Progress Series 434: 143–154.

508 Van Hoey, G., S. Degraer, & M. Vincx, 2004. Macrobenthic community structure of soft-bottom
509 sediments at the Belgian Continental Shelf. Estuarine, Coastal and Shelf Science 59: 599–613.

510 Vieira, A. R., A. Neves, V. Sequeira, R. B. Paiva, & L. S. Gordo, 2014. Otolith shape analysis as a tool for
511 stock discrimination of forkbeard (*Phycis phycis*) in the Northeast Atlantic. Hydrobiologia 728: 103–
512 110.

513 Vignon, M., & F. Morat, 2010. Environmental and genetic determinant of otolith shape revealed by a
514 non-indigenous tropical fish. Marine Ecology-progress Series 411: 231–241.

Tables

Table 1: Number of fish analyzed per station and per nursery (Belgian coast and Wadden Sea), including the date of capture, GPS coordinates, name of sampling survey (Demersal Young Fish Survey, DYFS, and B-FishConnect) and the sea surface temperature at the time of sampling are given

Year	Area	Coast side	Station	Sample size	Sampling date	GPS coordinates	Sea surface temperature (˚C)	Survey
2013	Belgium	West	OOST	14	28/08/2013	51.23 N, 2.80 E	19.3	B-FishConnect
			ST16	30	10/09/2013	51.19 N, 2.70 E	18.8	DYFS
		East	ST09	33	09/09/2013	51.35 N, 3.00 E	19.5	DYFS
			ST05	33	12/09/2013	51.45 N, 3.01 E	17.7	B-FishConnect
			ST37	29	12/09/2013	51.48 N, 3.14 E	17.8	DYFS
			ST06	14	13/09/2013	51.38 N, 2.85 E	17.7	DYFS
			FT02	20	24/09/2013	51.43 N, 3.31 E	16.9	DYFS
			Total	173				
2014	Belgium	West	ST23	30	15/09/2014	51.13 N, 2.70 E	18.1	DYFS
		East	ST09	27	16/09/2014	51.35 N, 3.00 E	18.5	DYFS
			FT01	23	10/10/2014	51.35 N, 3.10 E	16.9	B-FishConnect
			Total	80				
	Wadden Sea		NL01	34	16/09/2014	53.48 N, 6.49 E	18.2	DYFS
			NL02	27	23/09/2014	53.35 N, 6.97 E	18.1	DYFS
			Total	61				

515

Table 2: Summary of the mean value of the shape indices (form-factor, ellipticity and roundness) per size class for each dataset (n = 173 for BE2013, n = 80 for BE2014, n = 61 for NL2014) and comparisons of each shape index between the three different size classes (L1, L2 and L3) for each dataset and for the comparisons of all age-0 sole together at the regional (Belgian vs. Wadden Sea nursery) (n = 141) and at the local scale (Belgian 2013 vs. 2014) (n = 253), including the significance level

Shape indices	Datasets	L1 (52-76 mm)	L2 (76-82 mm)	L3 (82-102 mm)	L1-L2-L3 *P* value	All sizes	*P* value
Form-factor	BE2013	0.876	0.871	0.864	< 0.001	NL vs BE 2014	< 0.001
	BE2014	0.883	0.879	0.865	< 0.001		
	NL2014	0.874	0.860	0.855	< 0.01	BE 2013 vs 2014	< 0.01
Ellipticity	BE2013	0.039	0.043	0.048	0.016	NL vs BE 2014	0.723
	BE2014	0.034	0.038	0.047	0.012		
	NL2014	0.042	0.036	0.037	0.122	BE 2013 vs 2014	0.042
Roundness	BE2013	0.947	0.946	0.939	0.354	NL vs BE 2014	0.807
	BE2014	0.961	0.960	0.943	0.081		
	NL2014	0.946	0.958	0.953	0.102	BE 2013 vs 2014	0.005

516

Table 3: Summary of partial redundancy analysis (pRDA) for asymmetry (n = 314) and for spatio-temporal variations at the regional scale (Belgian vs. Wadden Sea nursery) (n = 141) and at the local scale (eastern vs. western coastal zones of the Belgian nursery and 2013 vs. 2014) (n = 253). Degrees of freedom (df), significance values and the variance explained by each variable (R^2) are included

Hypothesis	Factors	df	*P* value	R^2 adjusted (%)
Asymmetry: all otoliths	Otolith_side	1	0.01	5.8
Regional differences: NL-BE 2014	Nursery	1	0.04	0.6
	Sampling date	1	0.41	< 0
	SST	1	0.49	< 0
Local differences: BE 2013-2014	Year	1	0.08	< 0
	Sampling date	1	0.34	< 0
	East / West coastal regions	1	0.70	< 0
	SST	1	0.19	< 0

517

Figure captions

Figure 1: Map of the sampling stations of age-0 sole on the Belgian and the Wadden Sea nursery grounds in 2013 and 2014

Figure 2: Boxplot of form-factor (a) and ellipticity (b) for 314 age-0 sole juveniles of sole of three size classes for each dataset (n = 173 for BE2013, n = 80 for BE2014, n = 61 for NL2014)

Figure 3: Reconstruction of average sagittal otolith shape for 314 age-0 sole based on Elliptic Fourier Descriptors as a function of (**a**) otolith side (left dotted vs. right full line); (**b**) geography (Belgian nursery dotted vs. Wadden Sea full line); and (**c**) PCA clustering (Cluster 1 dotted vs. Cluster 2 full line see Figure 4 for the clusters). Non-overlapping regions of the otolith have been crosshatched to show differences between otolith shape

Figure 4: Principal Component Analysis of Fourier coefficients of otoliths of juvenile sole at (**a**) the regional scale (Belgian coast (●) vs. Wadden Sea nursery grounds (Δ)), and (**b**) at the local Belgian scale for the year 2013 (○) vs. 2014 (●)

Figure 5: Size distribution of the standard length (in mm) of the two clusters of sole sampled in 2014 on the Wadden Sea and Belgian nursery grounds (a) and on the Belgian nursery in 2013 and 2014 (b). The average standard length was significantly different between the two clusters (as indicated by the star in a) for the nursery comparison while it was not significantly (n.s.) different between the two clusters on the Belgian nursery (b)

518

Supplementary material

Figure S1: Cluster dendrogram of the similarity distances of the Fourier coefficients of ten randomly chosen otoliths of juvenile sole, based on Ward's distance. Picture numbers range from 1 to 40, with four consecutive pictures (e.g. 1-4, 5-8, etc.) being from the same otolith

Figure S2: Boxplot of roundness for 314 age-0 sole juveniles of sole at three size classes for each dataset (BE2013, BE2014 and NL2014)

Figure S3: Cluster dendrogram of the similarity distances of the Fourier coefficients of the juvenile sole sampled at the Belgian and Wadden Sea nursery grounds in 2014 (**a**) and at the Belgian nursery in 2013 and 2014 (**b**) using a complete hierarchical clustering method, based on Ward's distance

519

Figures

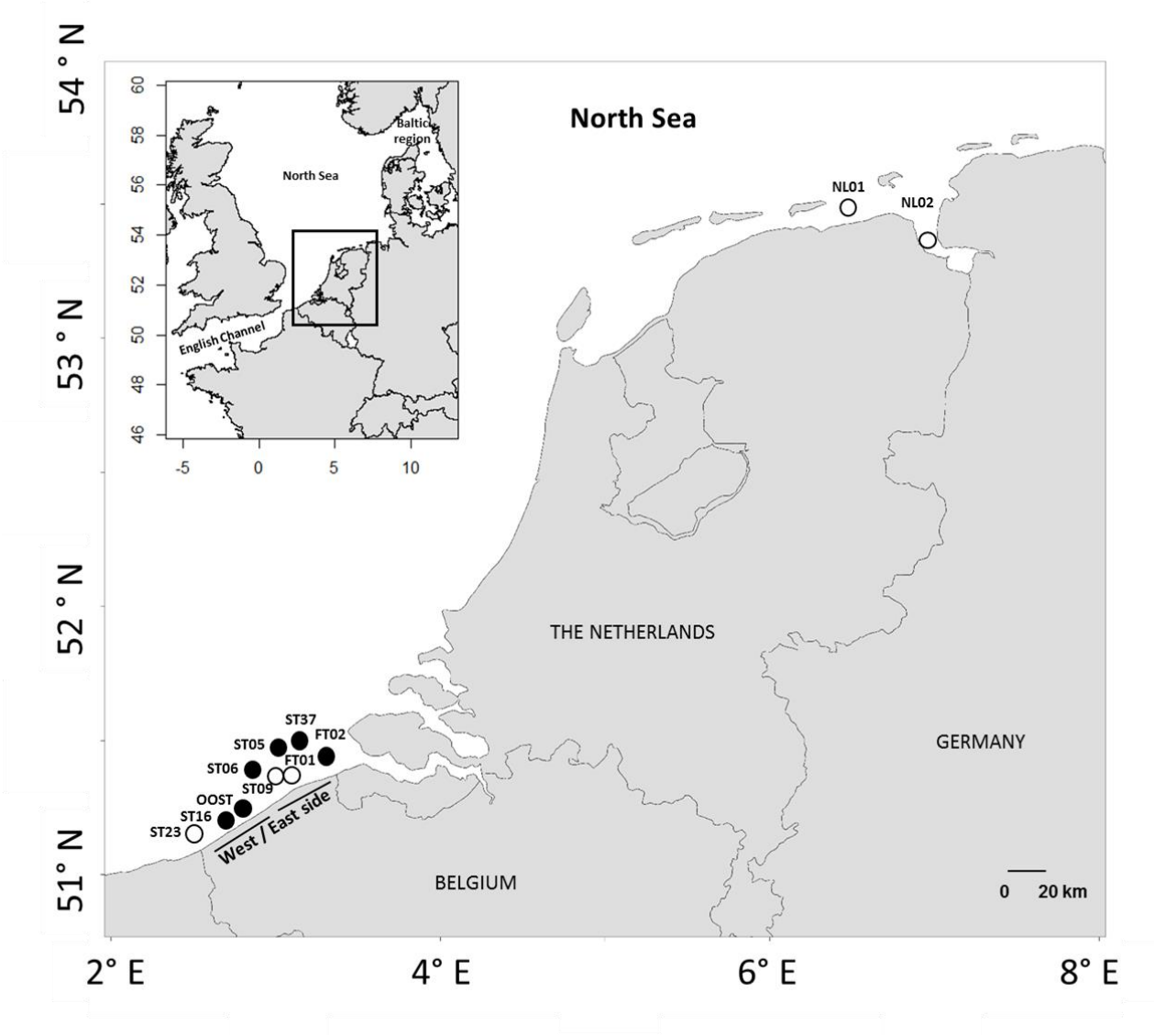

Figure 1: Map of the sampling stations of age-0 sole on the Belgian and the Wadden Sea nursery grounds in 2013 and 2014

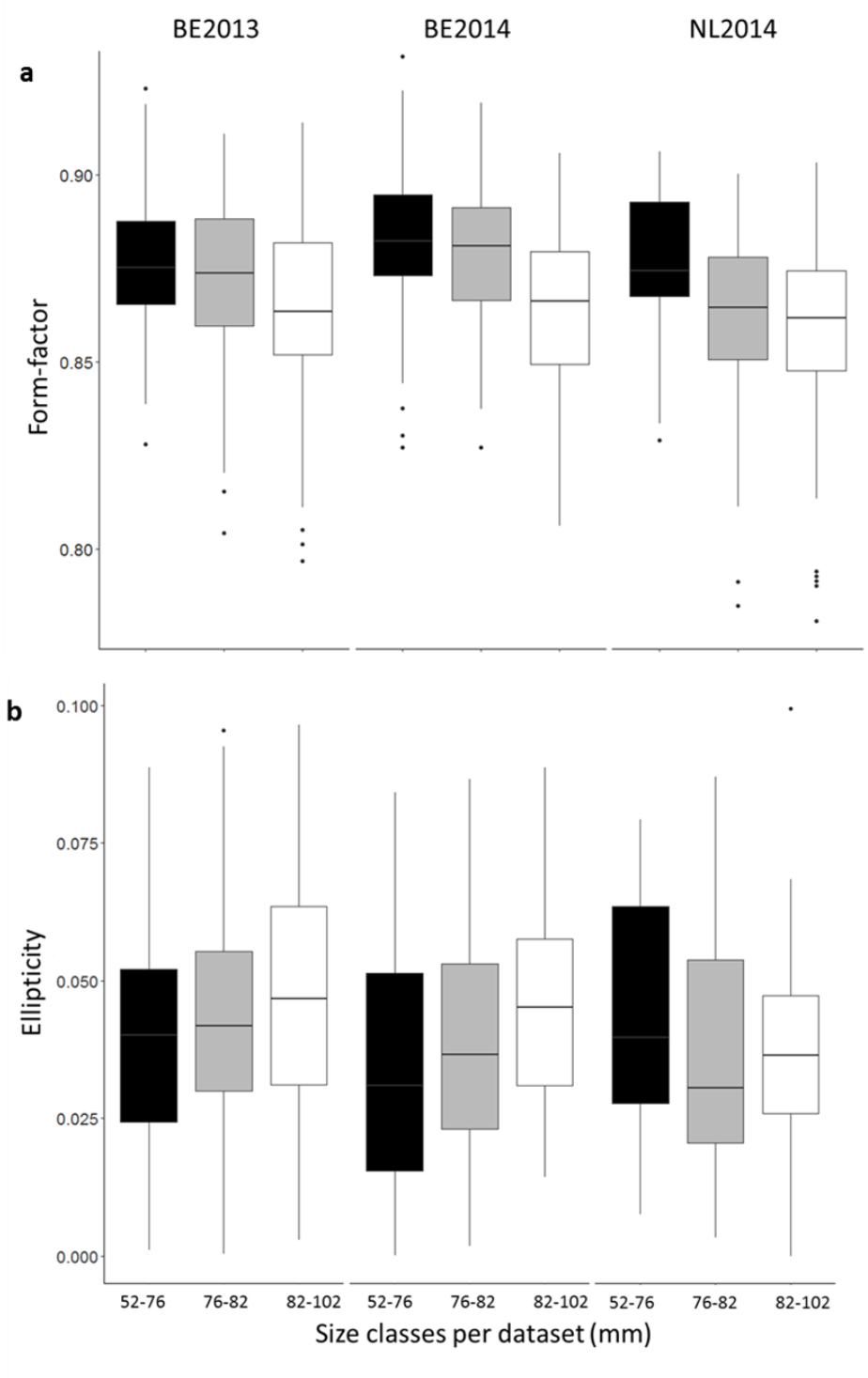

Figure 2: Boxplot of form-factor (a) and ellipticity (b) for 314 age-0 sole juveniles of sole of three size classes for each dataset (n = 173 for BE2013, n = 80 for BE2014, n = 61 for NL2014)

520

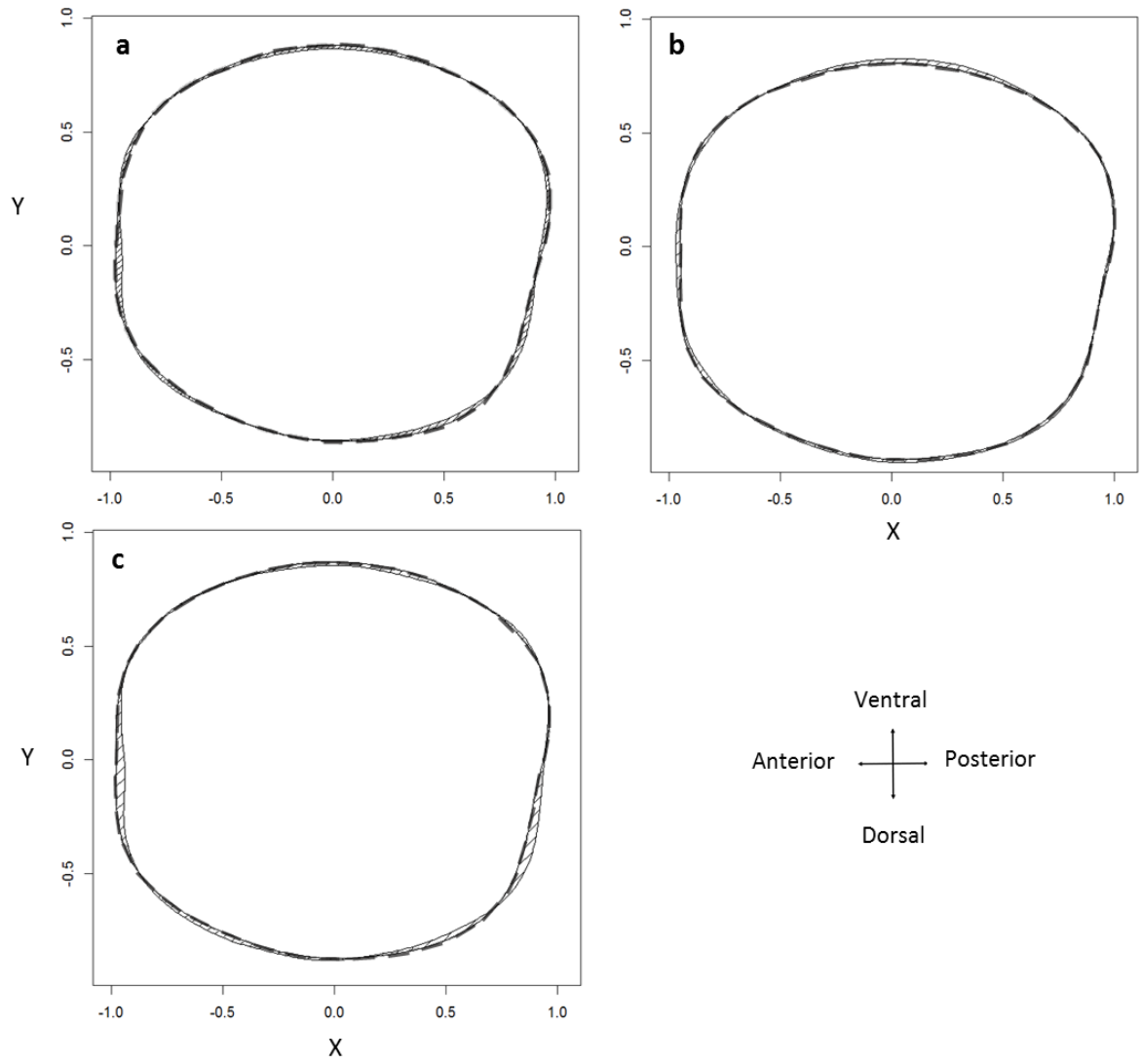

Figure 3: Reconstruction of average sagittal otolith shape for 314 age-0 sole based on Elliptic Fourier Descriptors as a function of (**a**) otolith side (left dotted vs. right full line); (**b**) geography (Belgian nursery dotted vs. Wadden Sea full line); and (**c**) PCA clustering (Cluster 1 dotted vs. Cluster 2 full line see Figure 4 for the clusters). Non-overlapping regions of the otolith have been crosshatched to show differences between otolith shape

521

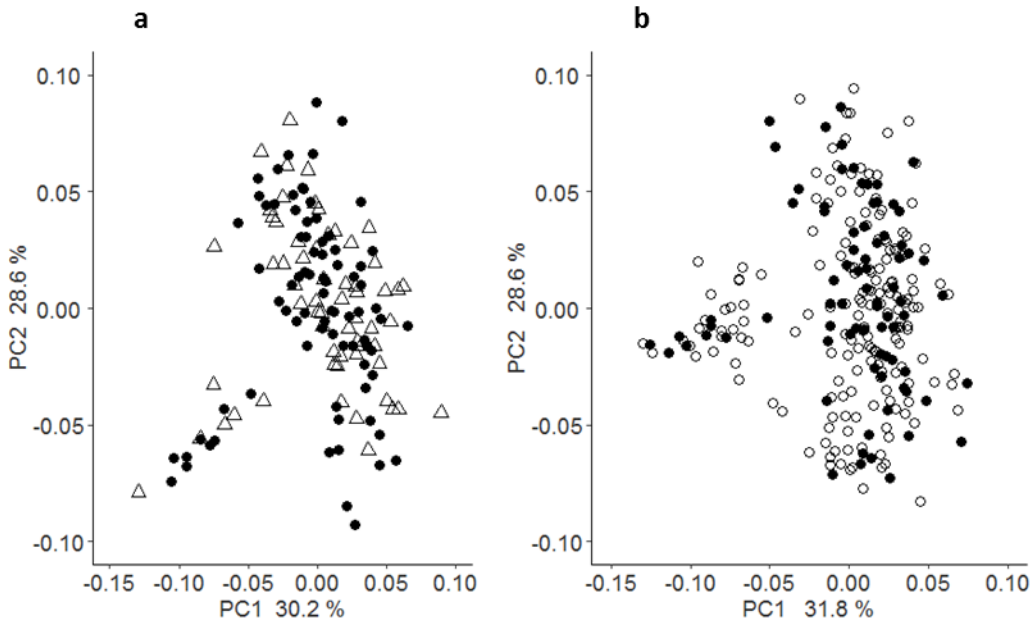

Figure 4: Principal Component Analysis of Fourier coefficients of otoliths of juvenile sole at (**a**) the regional scale (Belgian coast (●) vs. Wadden Sea nursery grounds (Δ)), and (**b**) at the local Belgian scale for the year 2013 (○) vs. 2014 (●)

522

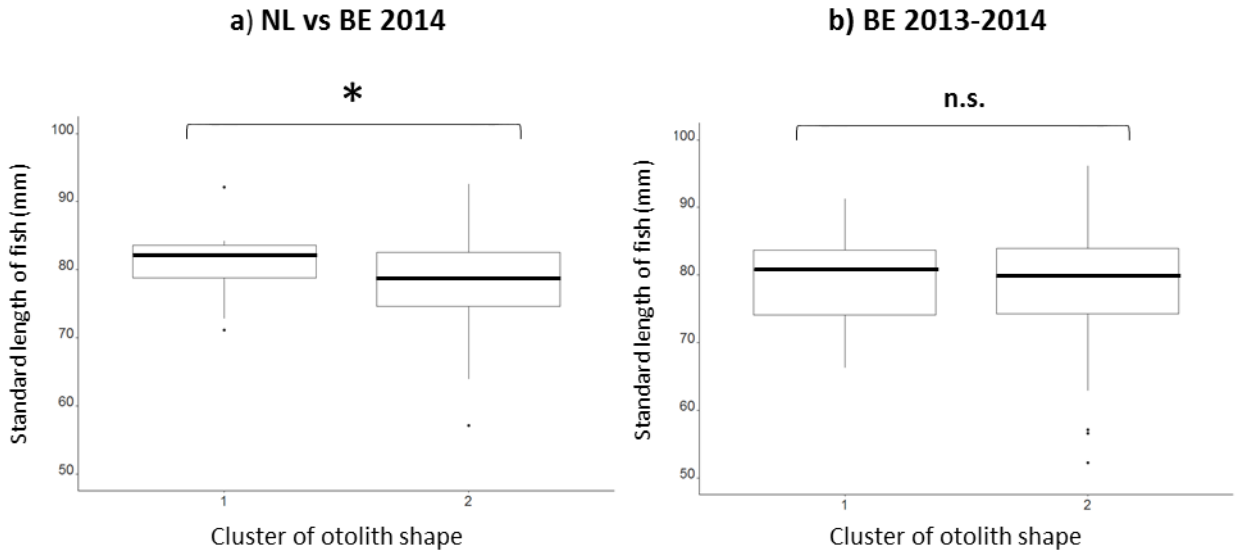

Figure 5: Size distribution of the standard length (in mm) of the two clusters of sole sampled in 2014 on the Wadden Sea and Belgian nursery grounds (a) and on the Belgian nursery in 2013 and 2014 (b). The average standard length was significantly different between the two clusters (as indicated by the star in a) for the nursery comparison while it was not significantly (n.s.) different between the two clusters on the Belgian nursery (b)

523

Table 1: Number of fish analyzed per station and per nursery (Belgian coast and Wadden Sea), including the date of capture, GPS coordinates, name of sampling survey (Demersal Young Fish Survey, DYFS, and B-FishConnect) and the sea surface temperature at the time of sampling are given

Year	Area	Coast side	Station	Sample size	Sampling date	GPS coordinates	Sea surface temperature (˚C)	Survey
2013	Belgium	West	OOST	14	28/08/2013	51.23 N, 2.80 E	19.3	B-FishConnect
			ST16	30	10/09/2013	51.19 N, 2.70 E	18.8	DYFS
		East	ST09	33	09/09/2013	51.35 N, 3.00 E	19.5	DYFS
			ST05	33	12/09/2013	51.45 N, 3.01 E	17.7	B-FishConnect
			ST37	29	12/09/2013	51.48 N, 3.14 E	17.8	DYFS
			ST06	14	13/09/2013	51.38 N, 2.85 E	17.7	DYFS
			FT02	20	24/09/2013	51.43 N, 3.31 E	16.9	DYFS
			Total	173				
2014	Belgium	West	ST23	30	15/09/2014	51.13 N, 2.70 E	18.1	DYFS
		East	ST09	27	16/09/2014	51.35 N, 3.00 E	18.5	DYFS
			FT01	23	10/10/2014	51.35 N, 3.10 E	16.9	B-FishConnect
			Total	80				
	Wadden Sea		NL01	34	16/09/2014	53.48 N, 6.49 E	18.2	DYFS
			NL02	27	23/09/2014	53.35 N, 6.97 E	18.1	DYFS
			Total	61				

524

Table 2: Summary of the mean value of the shape indices (form-factor, ellipticity and roundness) per size class for each dataset (n = 173 for BE2013, n = 80 for BE2014, n = 61 for NL2014) and comparisons of each shape index between the three different size classes (L1, L2 and L3) for each dataset and for the comparisons of all age-0 sole together at the regional (Belgian vs. Wadden Sea nursery) (n = 141) and at the local scale (Belgian 2013 vs. 2014) (n = 253), including the significance level

Shape indices	Datasets	L1 (52-76 mm)	L2 (76-82 mm)	L3 (82-102 mm)	L1-L2-L3 *P* value	All sizes	*P* value
Form-factor	BE2013	0.876	0.871	0.864	< 0.001	NL vs BE 2014	< 0.001
	BE2014	0.883	0.879	0.865	< 0.001		
	NL2014	0.874	0.860	0.855	< 0.01	BE 2013 vs 2014	< 0.01
Ellipticity	BE2013	0.039	0.043	0.048	0.016	NL vs BE 2014	0.723
	BE2014	0.034	0.038	0.047	0.012		
	NL2014	0.042	0.036	0.037	0.122	BE 2013 vs 2014	0.042
Roundness	BE2013	0.947	0.946	0.939	0.354	NL vs BE 2014	0.807
	BE2014	0.961	0.960	0.943	0.081		
	NL2014	0.946	0.958	0.953	0.102	BE 2013 vs 2014	0.005

525

Table 3: Summary of partial redundancy analysis (pRDA) for asymmetry (n = 314) and for spatio-temporal variations at the regional scale (Belgian vs. Wadden Sea nursery) (n = 141) and at the local scale (eastern vs. western coastal zones of the Belgian nursery and 2013 vs. 2014) (n = 253). Degrees of freedom (df), significance values and the variance explained by each variable (R^2) are included

Hypothesis	Factors	df	*P* value	R^2 adjusted (%)
Asymmetry: all otoliths	Otolith_side	1	0.01	5.8
Regional differences: NL-BE 2014	Nursery	1	0.04	0.6
	Sampling date	1	0.41	< 0
	SST	1	0.49	< 0
Local differences: BE 2013-2014	Year	1	0.08	< 0
	Sampling date	1	0.34	< 0
	East / West coastal regions	1	0.70	< 0
	SST	1	0.19	< 0

Supplementary material

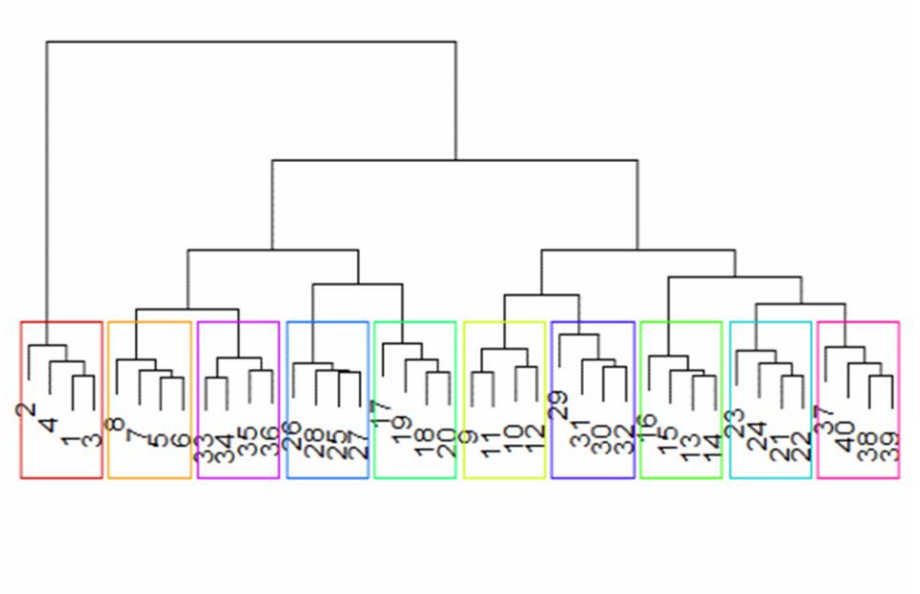

Figure S1: Cluster dendrogram of the similarity distances of the Fourier coefficients of ten randomly chosen otoliths of juvenile sole, based on Ward's distance. Picture numbers range from 1 to 40, with four consecutive pictures (e.g. 1-4, 5-8, etc.) being from the same otolith

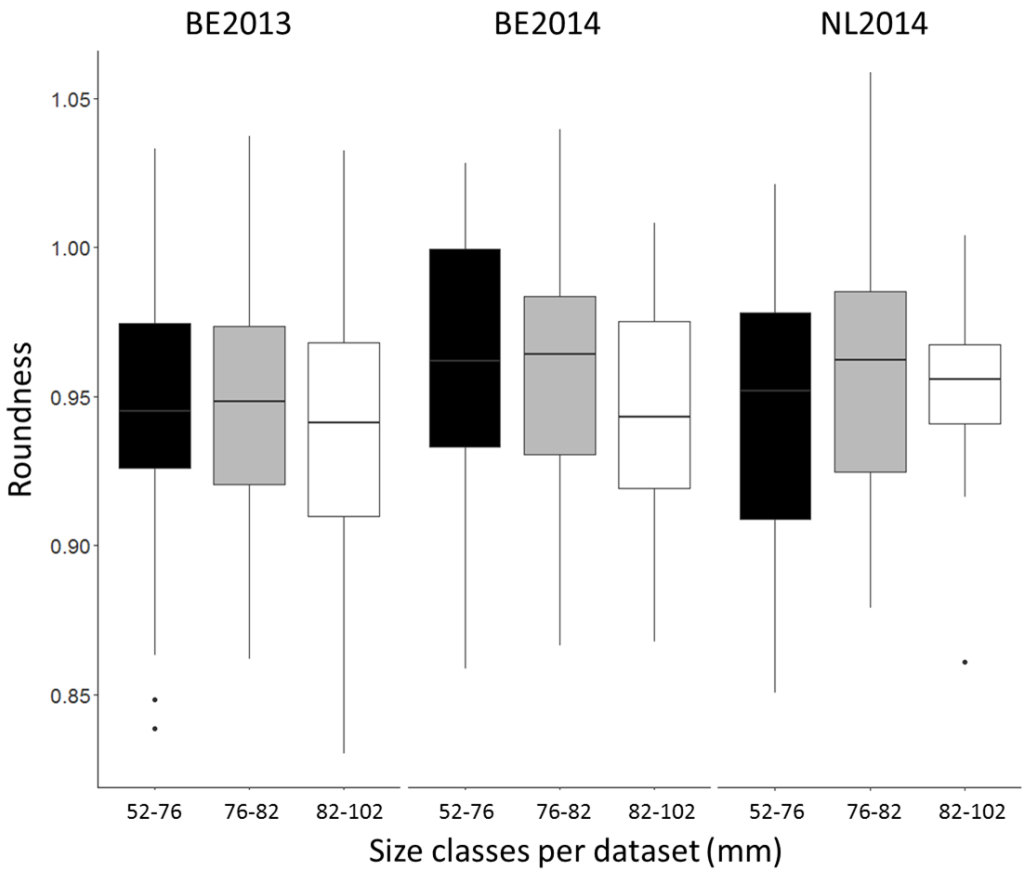

Figure S2: Boxplot of roundness for 314 age-0 sole juveniles of sole at three size classes for each dataset (BE2013, BE2014 and NL2014)

526

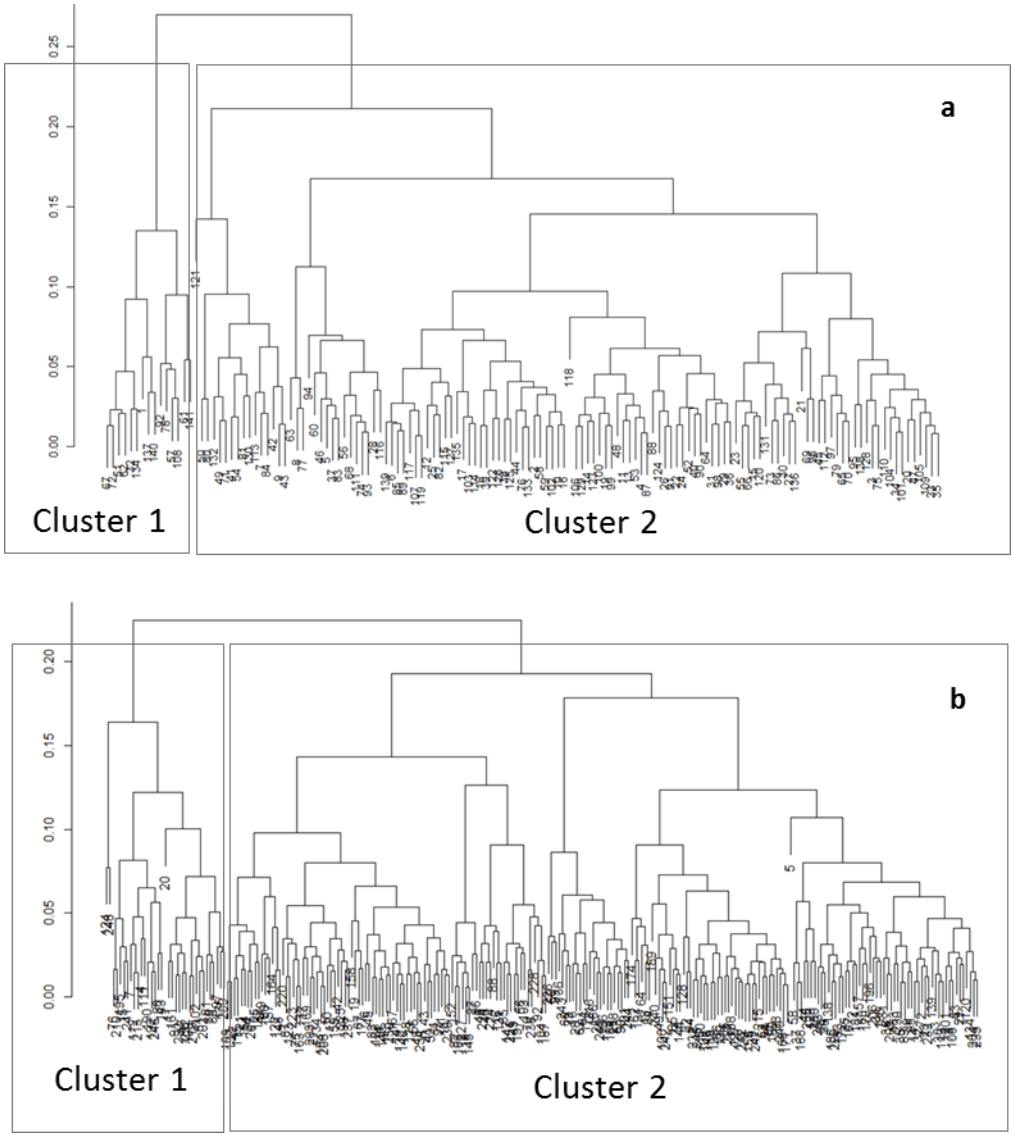

Figure S3: Cluster dendrogram of the similarity distances of the Fourier coefficients of the juvenile sole sampled at the Belgian and Wadden Sea nursery grounds in 2014 (**a**) and at the Belgian nursery in 2013 and 2014 (**b**) using a complete hierarchical clustering method, based on Ward's distance